# Simultaneous tracking and RSS model calibration by robust filtering

J. Manuel Castro-Arvizu[‡] , Jordi Vil-Valls[†], Pau Closas[†], Juan A. Fernández-Rubio[‡] [‡] Universitat Politècnica de Catalunya (UPC) Campus Nord, 08034 Barcelona (Spain)
[†]Centre Tecnològic de Telecomunicacions de Catalunya (CTTC) Av. Carl Friedrich Gauss 7, 08860 Castelldefels, Barcelona (Spain)

***Abstract*—Received Signal Strength (RSS) localization is widely used due to its simplicity and availability in most mobile devices. The RSS channel model is defined by the propagation losses and the shadow fading. These parameters might vary over time because of changes in the environment. In this paper, the problem of tracking a mobile node by RSS measurements is addressed, while simultaneously estimating a two-slope RSS model. The methodology considers a Kalman filter with Interacting Multiple Model architecture, coupled to an on-line estimation of the observation's variance. The performance of the method is shown through numerical simulations in realistic scenarios.**

## I. Introduction

The need for localization is not just confined to persons or vehicles of transportation in outdoor environments where Global Navigation Satellite Systems (GNSS) play an important role for this purpose. But accurately estimating location indoors, GNSS features remains a difficult problem because of signal blockage or severe attenuations.

Due to the present ubiquitous availability of powerful mobile computing devices, the bloom of personalized context- and localization-aware applications has become an active field of research. A way of localization in indoor environments is using signals of opportunity such as WLAN (IEEE 802.11x), Zigbee, UWB, etc. The advantage of working with signals of the IEEE 802.11 as the primary source of information to approach the localization problem is the inexpensive hardware and the already dense deployment of WLAN Access Points (APs) in urban areas.

The goal of this work is tracking a mobile path in a indoor environment using an existing WLAN infrastructure where several position-related measurements are available. Here we are interested in algorithms that use Received Signal Strength (RSS) observations for locating and tracking the mobile node, since most of mobile devices are equipped with wireless capability [1]. To achieve this aim in this work, a Kalman filtering is considered to perform the sequential tracking in a two-slope RSS model, for which we use an Interacting Multiple Model (IMM) architecture.

There are several channel models in the literature to characterize the indoor propagation environment [2], [3]. In this paper, the IEEE 802.11x model is considered because does not require an accurate floor plan of the indoor scenario and can be implemented without using a third party software [4].

This work uses the path loss two-slope model [5], that is a mathematical model of RSS and relates the path loss attenuation with distance. This means that the distance data between mobile target and the AP can be described by two models which depend of a breakpoint distance value. This channel model is used to design two kalman filters and an Interacting Multiple Model (IMM) is used to dynamically combine the outputs from two filters [6]. IMM technique is used to estimate the mode (mixing) probabilities for each model based Kalman filters and mix the two filter results based on the mode probabilities. Several works has used IMM techniques for location and control applications [7], [8], [9]

## II. System Model

We are interested in tracking a mobile device using RSS measurements from a set of $N$ APs. The estimation is performed in two steps: $i$) estimation of relative distances to the set of visible APs; $ii$) fusion of these distance measurements into a blended tracking solution. In this section, we present the peculiarities of the two-slope RSS model and the state-space formulation of the distance estimation problem.

### A. Two-slope RSS model

The widely used model for RSS observations is the path loss model, which is a simple yet realistic model for such measurements. It is parameterized by the path loss exponent (related to the power decay with respect to distance) and the shadowing (that is, the random propagation effects). However, it has been observed in experimental campaigns that these parameters fluctuate and are indeed distance dependant. As a conclusion, the parameters employed in the traditional path loss model are highly site-specific [10] [11]. Therefore, in many situations more sophisticated models should be accounted.

In this work we consider an extension of the classical path loss model accounting for two regions of propagation, referred

This work has been partially supported by the Spanish Ministry of Economy and Competitiveness project TEC2012-39143 (SOSRAD), by the European Commission in the Network of Excellence in Wireless COMmunications NEWCOM♯ (contract n. 318306), and by Generalitat de Catalunya under grant 2014-SGR-1567. This work is also supported by the "Ministerio de Economa y Competitividad" of the Spanish Government and ERDF funds (TEC2013-41315-R DISNET), the Catalan Government (2014 SGR 60 AGAUR) and the National Council of Science and Technology (CONACyT) of the Mexican Government

to as the two-slope model [5]. Path loss refers to the average loss in signal strength over distance. For indoor environments, the path loss depends on the relative distance between the AP and the sensing device [12]. For far distances (e.g., $5 \geq d \geq 30$ meters), path reflections from the environment (specially reflections from surrounding walls) generally result in a steeper overall drop in the signal strength at the receiver. Under this model, the RSS for the $r$-th AP ($r = 1, 2, \ldots, N$ total number of APs) to the mobile target is modeled as [5]:

$$\mathrm{RSS}^r(d) = \begin{cases} h^{(1)}(d) + \chi_{\sigma_1^2} & \text{if } d \leq d_{bp} \\ h^{(2)}(d) + \chi_{\sigma_2^2} & \text{if } d > d_{bp} \end{cases} \quad (1)$$

where $d$ is the relative distance between the AP and the moving node were the RSS was measured, and

$$h^{(1)}(d) = 10\alpha_1 \log_{10}(d) \quad (2)$$

$$h^{(2)}(d) = 10\alpha_1 \log_{10}(d_{bp}) + 10\alpha_2 \log_{10}(d/d_{bp}) \ . \quad (3)$$

The first equation gives the path loss (in decibels) for close distances (distances less than $d_{bp}$, known as the breakpoint distance) and the second equation gives the path loss beyond $d_{bp}$. The $\alpha_1$ and $\alpha_2$ values are the path loss exponents, defining the slopes before and after $d_{bp}$, respectively. The functions $h^{(1)}(d)$ and $h^{(2)}(d)$ were obtained by measurement campaigns using radio signal ray tracing methods, premeasured RSS contours centered in the receiver or multiple measurements at several base stations [1], [13], [14].

Depending on the transmitter/receiver geometrical configuration, the RSS measurements might be distorted from the nominal. This variation (known as shadow fading or log-normal shadowing) can be modeled by an additive zero-mean Gaussian random variable. The notation, $\chi_{\sigma^2} \sim \mathcal{N}(0, \sigma^2)$ is used. As happens for the path loss exponents, the variance values differ before and after the breakpoint distance. Typically the values depend on the scenario but in all cases it is observed that $\sigma_1^2$ ¡ $\sigma_2^2$ and $\alpha_1$ ¡ $\alpha_2$. The standard deviation of the received power before and after breakpoint distance, $\sigma_1$ and $\sigma_2$, is expressed in units of dB and is assumed relatively constant with distance. Figure 1 represents a simulation of real measurements taken from the two-slope path loss model at different relative distances between one AP and the mobile target.

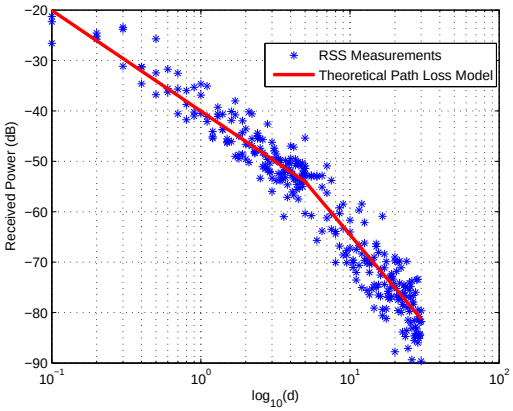


Fig. 1. Simulation of a two-slope path loss model with $\sigma_1$ = 3 dB, $\sigma_2$= 5 dB, $\alpha_1$=2, $\alpha_2$=3.5, and $d_{bp} = 5$ meters.

### *B. State-space model*

As previously stated, the proposed strategy to solve the localization problem uses a two-step approach. In the first step (i.e., distance estimation) and for the $r^{th}$ AP, the observations correspond to the RSS measurements and the unknown states to be sequentially inferred are

$$\boldsymbol{\theta}_k^r = \begin{bmatrix} d_k^r & \dot{d}_k^r \end{bmatrix}^T \quad (4)$$

where $d_k^r$ is the distance between the mobile and the $r$-th AP and $\dot{d}_k^r$ is the rate of change of this distance. We assume a linear evolution of states in the form of

$$\boldsymbol{\theta}_k^r = \mathbf{A}\boldsymbol{\theta}_{k-1}^r + \mathbf{B}v_k^r \quad (5)$$

where $\mathbf{B}v_k^r$ is the process noise accounting for possible modeling mismatches, such as a possible acceleration of the mobile. In other words, this noise term gathers different forces that could affect target's dynamics and which are not explicitly modeled. The process noise is normally distributed with zero mean and covariance matrix $\mathbf{Q}_k$ [15]:

$$\mathbf{Q}_k = \sigma_d^2 \mathbf{B}\mathbf{B}^T \quad (6)$$

where $\sigma_d^2$ models the uncertainty on the mobile dynamics.The state equation includes these matrices:

$$\mathbf{A} = \begin{bmatrix} 1 & \Delta t \\ 0 & 1 \end{bmatrix} \ ; \ \mathbf{B} = \begin{bmatrix} \frac{\Delta t^2}{2} \\ \Delta t \end{bmatrix} \quad (7)$$

where $\Delta$t is the sampling period.

To complete the state-space representation, the observation vector is defined. In this case, the RSS measurements per AP are precisely the observations used to infer $\boldsymbol{\theta}_k^r$, and thus

$$z_k^r \triangleq \mathrm{RSS}^r(d_k) = h(d_k) + n_k \quad (8)$$

where we recall that the model for $\mathrm{RSS}^r(d)$ depends on the breakpoint distance. Therefore, $h(\cdot)$ has to be selected according to (1) and the statistics of the measurement noise as well, that is whether its variance is $\sigma_1^2$ or $\sigma_2^2$.

In this work, a solution involving an Extended Kalman filter (EKF) is considered to deal with the nonlinear filtering problem, for which we have to derive the Jacobian matrix of the measurements function because $h^{(1)}$ and $h^{(2)}$ are nonlinear. The $2 \times 1$ Jacobian matrices $\mathbf{H}_k^{(1)}$ and $\mathbf{H}_k^{(2)}$ are

$$\mathbf{H}_k^{(1)} = \begin{bmatrix} \frac{\alpha_1}{\log 10} \frac{10}{d} & 0 \end{bmatrix} \ ; \ \mathbf{H}_k^{(2)} = \begin{bmatrix} \frac{\alpha_2}{\log 10} \frac{10}{d} & 0 \end{bmatrix} \ . \quad (9)$$

## III. Interactive Multiple Model Approach

The main goal in the RSS-based localization problem is to infer the distance to each AP, and the corresponding distance rate, from a set of $N$ RSS measurements. The main concern of this section is to present and justify the reasoning behind the use of an IMM-based approach to solve such problem.

### A. Parallel IMM-based solution

The first approach that comes to mind to solve this problem is the use of a traditional filtering solution, such as the EKF, where the observation accounts for the full set of RSS measurements $\mathbf{z}_k = [z_k^1, ..., z_k^N]^T$ and the global state evolution takes into account the $N$ individual states, $\boldsymbol{\theta}_k = [\boldsymbol{\theta}_k^1; ...; \boldsymbol{\theta}_k^N]$ . But it is straightforward to see from (1) that this is not a valid approach, because the measurement model directly depends on the breakpoint distance. The two-slope model can be used to model the distance between the AP and the mobile node but both implicit models must be treated separately. The natural solution to overcome this model-switching problem is to use an IMM-based approach.

The key idea behind the IMM is to use a bank of $M$ KFs, each one designed to cope with a specific model (or model set), and to obtain the state estimation as a clever combination of the individual estimates. If the full set of $N$ independent observations $\mathbf{z}_k$ is considered, the question that arises is how many KFs should be considered into the IMM As each independent observation may obey model 1 or model 2, the answer is $2^N$ filters (i.e., all the possible combinations of model 1 and 2 for the $N$ observations). It is clear that this is not a practical solution for an arbitrary number of APs, therefore, a divide-and-conquer strategy treating independent measurements separately is the best solution. In this contribution a parallel IMM-based approach is adopted, considering $N$ IMMs each one involving 2 KFs according to the two path loss models (shown in Figure 2).

At each discrete-time instant $k$, the IMM algorithm follows a clear three step architecture: *Reinitialization*, *KF* and *Model probability*. The final estimates are obtained as a combination of the individual KF outputs using the corresponding model likelihoods. Mathematically, one cycle of the standard IMM associated to the $r^{th}$ RSS measurement is sketched in Algorithm 1, where $\pi_{ji}$ (for $i, j = 1, 2$) is a two-state Markov model transition probability matrix and is set in the proposed algorithm as,

$$\pi_{ji} = \begin{bmatrix} 0.9995 & 0.005 \\ 0.005 & 0.9995 \end{bmatrix} \tag{10}$$

for each AP.

Notice that in its standard form, both the two-slope model parameters and the process noise variance, gathered in vector $\boldsymbol{\psi}^{(1)}$, must be specified in the IMM. These parameters must be set to the true ones for an optimal solution. Moreover, the initialization of both EKFs and each AP, $\left\{\hat{\boldsymbol{\theta}}_{0|0}^{(i),r}, \mathbf{P}_{0|0}^{(i),r} \text{ for } i = 1, 2\right\}$, must be set according to the problem at hand. The error covariance matrix has a initial value assigned as $\mathbf{P}_{0|0}^{(i),r} = 4\mathbf{Q}_k$ for each AP. The initial value state vector for the filter is $\hat{\boldsymbol{\theta}}_{0|0}^{(i),r}$=$\boldsymbol{\theta}_0^r + \boldsymbol{\omega}$ where $\boldsymbol{\omega} \sim \mathcal{N}(\mathbf{0}, 0.8\boldsymbol{I}_2)$. The initial model probabilities are set as $\eta_{(1),k}^r = \eta_{(2,)k}^r = 0.5$ for every AP also.

### B. Location Calculation Model

The final goal is to sequentially obtain the mobile position. The location calculation is solved with a KF using the $N$ distance estimates obtained from the bank of IMMs as observations (see Figure 2). In the following, the location calculation model is detailed:

The state vector gathers the mobile position and velocity, $\boldsymbol{x}_k = [x_k, y_k, \dot{x_k}, \dot{y_k}]$, and the observations vector is defined as

$$\mathbf{z}_k^d = \begin{bmatrix} d_{1,k} & ... & d_{N,k} \end{bmatrix} \tag{23}$$

where $\hat{\boldsymbol{\theta}}_{k|k}^r(1) \triangleq d_{r,k}$ is the distance obtained from the $r^{th}$ IMM. The state equation is

$$\boldsymbol{x}_k = \mathbf{A}_{pos}\mathbf{x}_{k-1} + \mathbf{B}_{pos}w_k \tag{24}$$

where the resulting Gaussian process noise has a covariance matrix $\mathbf{Q}_{pos,k} = \sigma_p^2 \mathbf{B}_{pos}\mathbf{B}_{pos}^T$, $\sigma_p^2$ is the variance related to

**Algorithm 1** Cycle $k$ of the IMM for the $r^{th}$ AP

1: For $i = 1, 2$ and $j = 1, 2$

2: **Reinitialization**:

Calculation of the predicted mode probability, mixing weights, mixing estimates and mixing covariances, respectively,

$$\eta_{k|k-1}^{(i),r} = \sum_j \pi_{ji}\eta_{k-1}^{(j),r} \; ; \; \eta_{k-1}^{j|i,r} = \frac{\pi_{ji}\eta_{k-1}^{(j),r}}{\eta_{k|k-1}^{(i),r}} \tag{11}$$

$$\bar{\boldsymbol{\theta}}_{k-1|k-1}^{(i),r} = \sum_j \hat{\boldsymbol{\theta}}_{k-1|k-1}^{(j),r}\eta_{k-1}^{j|i,r} \tag{12}$$

$$\bar{\mathbf{P}}_{k-1|k-1}^{(i),r} = \sum_j [\mathbf{P}_{k-1|k-1}^{(j),r} + (\bar{\boldsymbol{\theta}}_{k-1|k-1}^{(i),r} - \hat{\boldsymbol{\theta}}_{k-1|k-1}^{(j),r}) \times (\bar{\boldsymbol{\theta}}_{k-1|k-1}^{(i),r} - \hat{\boldsymbol{\theta}}_{k-1|k-1}^{(j),r})']\eta_{k-1}^{j|i,r} \tag{13}$$

3: **Model-conditioned std. KF**:
Prediction, innovations' covariance matrix, Kalman gain, state estimate and the corresponding error covariance matrix, are given by

$$\hat{\boldsymbol{\theta}}_{k|k-1}^{(i),r} = \mathbf{A}\bar{\boldsymbol{\theta}}_{k-1|k-1}^{(i),r} \; ; \; \mathbf{P}_{k|k-1}^{(i)} = \mathbf{A}\bar{\mathbf{P}}_{k-1|k-1}^{(i),r}\mathbf{A}^T + \mathbf{Q}_k^{(i)} \tag{14}$$

$$S_k^{(i),r} = \mathbf{H}_k^{(i),r}\mathbf{P}_{k|k-1}^{(i),r}(\mathbf{H}_k^{(i),r})^T + R^{(i)} \tag{15}$$

$$\mathbf{K}_k^{(i),r} = \mathbf{P}_{k|k-1}^{(i),r}(\mathbf{H}_k^{(i),r})^T(S_k^{(i),r})^{-1} \tag{16}$$

$$\hat{\boldsymbol{\theta}}_{k|k}^{(i),r} = \hat{\boldsymbol{\theta}}_{k|k-1}^{(i),r} + \mathbf{K}_k^{(i),r}(z_k^r - \mathbf{H}_k^{(i),r}\hat{\boldsymbol{\theta}}_{k|k-1}^{(i),r}) \tag{17}$$

$$\mathbf{P}_{k|k}^{(i),r} = \mathbf{P}_{k|k-1}^{(i),r} - \mathbf{K}_k^{(i),r}S_k^{(i),r}(\mathbf{K}_k^{(i),r})^T \tag{18}$$

4: **Model probability update**:
The model likelihood function and model probability are respectively

$$L_k^{(i),r} = \mathcal{N}(\tilde{z}_k^{(i),r}; 0, S_k^{(i),r}) \tag{19}$$

$$\eta_k^{(i),r} = \frac{\eta_{k|k-1}^{(i),r}L_k^{(i),r}}{\sum_j \eta_{k|k-1}^{(j),r}L_k^{(j),r}} \tag{20}$$

5: **Estimate fusion**:

$$\hat{\boldsymbol{\theta}}_{k|k}^r = \sum_i \hat{\boldsymbol{\theta}}_{k|k}^{(i),r}\eta_k^{(i),r} \tag{21}$$

$$\mathbf{P}_{k|k}^r = \sum_i [\mathbf{P}_{k|k}^{(i),r} + (\hat{\boldsymbol{\theta}}_{k|k}^r - \hat{\boldsymbol{\theta}}_{k|k}^{(i),r})(\hat{\boldsymbol{\theta}}_{k|k}^r - \hat{\boldsymbol{\theta}}_{k|k}^{(i),r})']\eta_k^{(i),r} \tag{22}$$

the mobile acceleration, and

$$\mathbf{A}_{pos} = \begin{bmatrix} 1 & 0 & \Delta t & 0 \\ 0 & 1 & 0 & \Delta t \\ 0 & 0 & 1 & 0 \\ 0 & 0 & 0 & 1 \end{bmatrix} \; ; \; \mathbf{B}_{pos} = \begin{bmatrix} \frac{\Delta t}{2} & 0 \\ 0 & \frac{\Delta t}{2} \\ \Delta t & 0 \\ 0 & \Delta t \end{bmatrix} . \quad (25)$$

The observation equation is

$$\mathbf{z}_k^d = \mathbf{h}_k(\boldsymbol{x}_k) + \boldsymbol{\nu}_k \quad (26)$$

where the observation error is modeled as an uncorrelated white Gaussian noise with covariance $\mathbf{R}_{pos,k} = \text{diag}(\mathbf{P}_{k|k}^1(1,1), ..., \mathbf{P}_{k|k}^N(1,1))$, the nonlinear observation function $\mathbf{h}_k(\mathbf{x}_k)$ is defined as the distance of the mobile to every anchor point,

$$\mathbf{h}_k = \begin{bmatrix} \sqrt{(x_k - x_p^1)^2 + (y_k - y_p^1)^2} \\ \vdots \\ \sqrt{(x_k - x_p^N)^2 + (y_k - y_p^N)^2} \end{bmatrix} = \begin{bmatrix} d_{m\to 1} \\ \vdots \\ d_{m\to N} \end{bmatrix}, \quad (27)$$

where $\{x_p^r, y_p^r\}$ is the position of the $r^{th}$ AP, and the jacobian used to implement the EKF is given by

$$\mathbf{H}_k = \begin{bmatrix} \frac{x_k - x_p^1}{d_{m\to 1}} & \frac{y_k - y_p^1}{d_{m\to 1}} & 0 & 0 \\ \vdots & & & \vdots \\ \frac{x_k - x_p^N}{d_{m\to N}} & \frac{y_k - y_p^N}{d_{m\to N}} & 0 & 0 \end{bmatrix} \Bigg|_{\mathbf{x}_k = \hat{\mathbf{x}}_{k|k-1}} .$$

The initial value state vector for the filter is $\hat{\boldsymbol{x}}_{0|0} = \boldsymbol{x}_0 + \boldsymbol{\omega}$, with $\boldsymbol{\omega} \sim \mathcal{N}(\mathbf{0}, 0.8\boldsymbol{I}_4)$.

## IV. Maximum Likelihood Covariance estimator for model calibration

In the two-slope model (1), the RSS measurements may come from the first equation modeling the propagation for close distances or alternatively, they may obey the second equation modeling the propagation for distances beyond the breakpoint distance.

In the proposed methodology, each IMM inherently treats this model uncertainty by computing the model likelihood from the innovations of each KF. For each AP $r$ and model $i$, the model probability is given by $\eta_k^{(i),r}$. These probabilities are used into the filter to weight the outputs of the individual KFs but can also be reused for the model calibration. At each time step and using these model probabilities, two subsets of RSS measurements are constructed: if $\eta_k^{(1),r} > \eta_k^{(2),r}$, the RSS measurement $y_k^r$ is associated to $y_{1,k}^r$ (i.e., which represents the RSS measurements subset obeying $\mathcal{Y}_1$,

$$\mathcal{Y}_{1,k}^r = \{y_k^r \; : \; \eta_k^{(1),r} > \eta_k^{(2),r}\} \; , \quad (28)$$

otherwise, it is associated to $\mathcal{Y}_{2,k}^r$ (i.e., which concatenates the RSS measurements obeying $\mathcal{Y}_2$). For the sake of clarity in the forthcoming derivations, the elements in the sets are defined as

$$\mathcal{Y}_{1,k}^r = \{y_{1,1}^r, \ldots, y_{1,L_1}^r\} \quad (29)$$
$$\mathcal{Y}_{2,k}^r = \{y_{2,1}^r, \ldots, y_{2,L_2}^r\} \; . \quad (30)$$

For the $r^{th}$ AP, the $\ell^{th}$ sample of the first model subset $\mathcal{Y}_{1,k}^r$ at time $k$ is Gaussian distributed,

$$y_{1,\ell}^r \sim \mathcal{N}(\bar{y}_{1,\ell}^r, \sigma_1^{2,r}), \quad (31)$$

with $\bar{y}_{1,\ell}^r = L_0 + 10\alpha_{1,1}^r \log_{10} d_\ell^r$.

Using this subset and assuming a known distance to the $r^{th}$ AP, $d_\ell^r$, at instant $k$ the ML $\sigma_1^2$ estimator is given by

$$\hat{\sigma}_1^{2,r} = \frac{1}{L_1} \sum_{\ell=1}^{L_1} \left(y_{1,\ell}^r - \bar{y}_{1,\ell}^r\right)^2 \quad (32)$$

The ML estimator for $\sigma_2^2$ follows the same procedure but using the second model subset of RSS measurements. For the $r^{th}$ AP, the $\ell^{th}$ sample of the second model subset $\mathcal{Y}_{2,k}^r$ at time $k$ is Gaussian distributed as well,

$$y_{2,\ell}^r \sim \mathcal{N}(\bar{y}_{2,\ell}^r, \sigma_2^{2,r}), \quad (33)$$

with $\bar{y}_{2,\ell}^r = L_0 + 10\alpha_{1,2}^r \log_{10} d_{bp} + 10\alpha_2^r \log_{10}\left(\frac{d_\ell^r}{d_{bp}}\right)$.

Using this subset and assuming a known distance to the $r^{th}$ AP, $d_\ell^r$, then at time instant $k$ the ML estimator of $\sigma_2^2$ is given by

$$\hat{\sigma}_2^2 = \frac{1}{L_2} \sum_{\ell=1}^{L_2} \left(y_{2,\ell}^r - \bar{y}_{2,\ell}^r\right)^2 , \quad (34)$$

## V. Results

The first approach in this work was estimating the distance to every AP in every $k$ instant. A single realization was performed and the figure 3 shows $\theta_k^1$[1,0], illustrating the case when the mobile node is close to the breakpoint distance. When this happens, the model probabilities $\eta_k^{(1),r}$ and $\eta_k^{(2),r}$ exhibit nervous behaviors. The estimated distance referred in figure 3 corresponds to AP number 5. The top plot presents the estimated distance and the bottom plot shows the performance of the decision process in $\mathcal{Y}_1$-$\mathcal{Y}_2$ switching.

The IMM performance was evaluated with the RMSE values. Focusing in AP 5 as an illustrative example, the RMSE for $\sigma_1$ and $\sigma_2$ is shown in Figure 4 where is observed the convergence of our algorithm after some instants.

The bottom plot in the figure 5 shows the average RMSE of the distance over all 6 APs. The top plot illustrates the corresponding RMSE of position estimation. From this figure, it is notable that the IMM algorithm implemented under covariance estimation has good accuracy in terms of mobile location.

The calibration performance is also demonstrated in figure 6. Being in the case when the mobile is close or under the breakpoint distance (that is the border for the two-slope model), the mixing probability $\eta_k^{(i)}$ is plotted and the performance of $\sigma_1$ and $\sigma_2$ in every $k$ also. This plot is for only one AP and for the

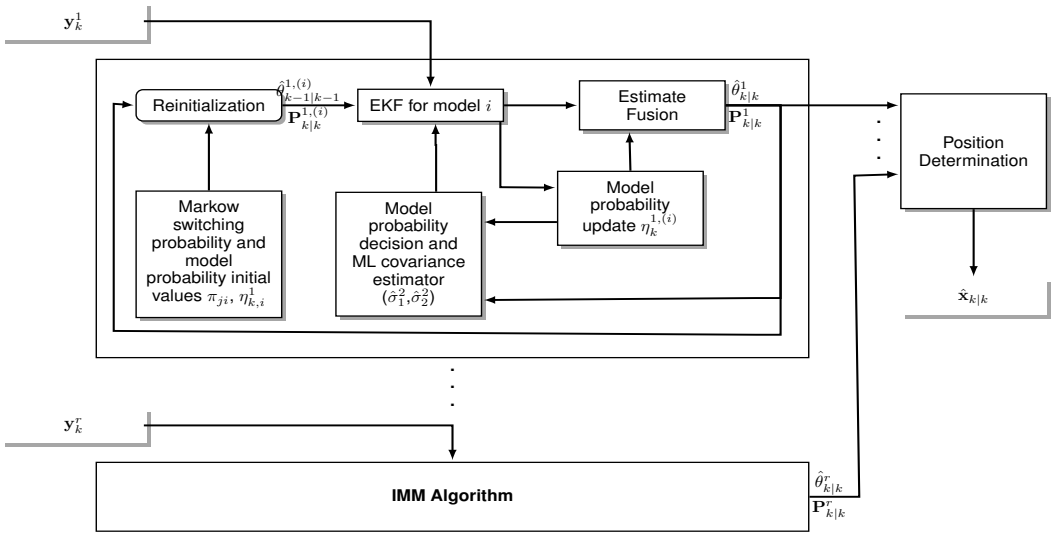


Fig. 2. Complete IMM Architecture with parameters estimation for every $k$ instant.

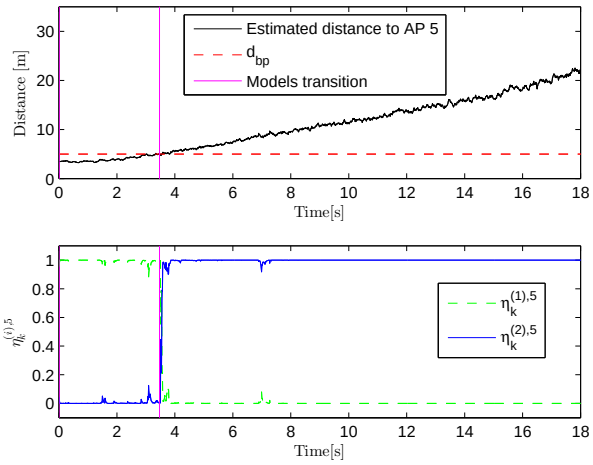


Fig. 3. Estimated distance according to probability performance $\eta_k^1$ to AP 5 for one realization.

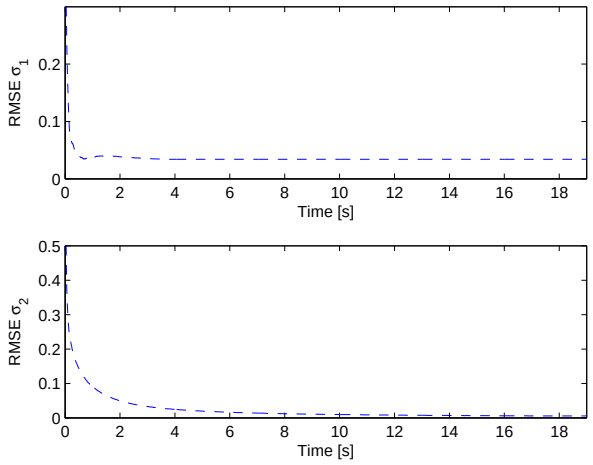


Fig. 4. RMSE of the estimation of $\sigma_1$ and $\sigma_2$ with AP 5.

case when the mobile moves close to the breakpoint distance value.

The final result of this work for a long trajectory is shown in figure 7. This simulation gives a good estimation for the mobile's path.

## VI. Conclusions

The mobile location via RSS measurements and the covariance calibration in a realistically wireless scenario has been formulated as a switching non-linear state problem. This work proposes an EK-IMM algorithm to face the problem when the mobile is switching of a model to other. With the aid of the likelihood function, the proposed method determines the probabilities of the two models and so accurate a distance between the mobile and the Anchor Point. Simulation results shows that the EK-IMM algorithm gives a good mobile location estimation alike the covariance calibration of the channel. However the path-loss model parameters and $d_{bp}$ are possible to estimate using the same EK-IMM algorithm but the computational complexity could increase. For this reason, using other smoothing algorithms are recommended as future work.

## References

[1] Theodore Rappaport, *Wireless Communications: Principles and Practice*, Prentice Hall PTR, Upper Saddle River, NJ, USA, 2nd edition, 2001.

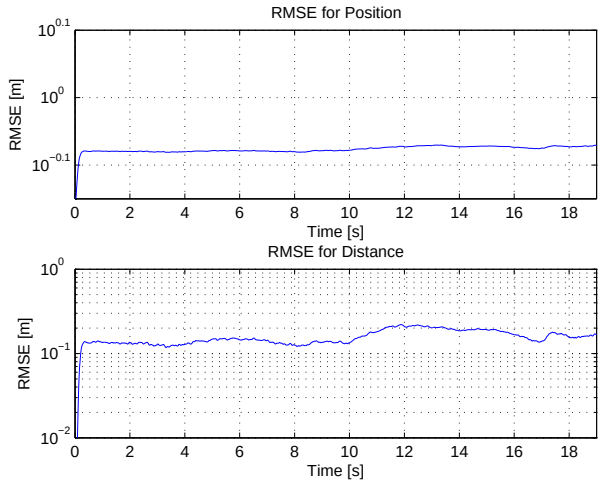


Fig. 5. Average RMSE of the distance between Mobile target and every AP and RMSE performance of the position estimation.

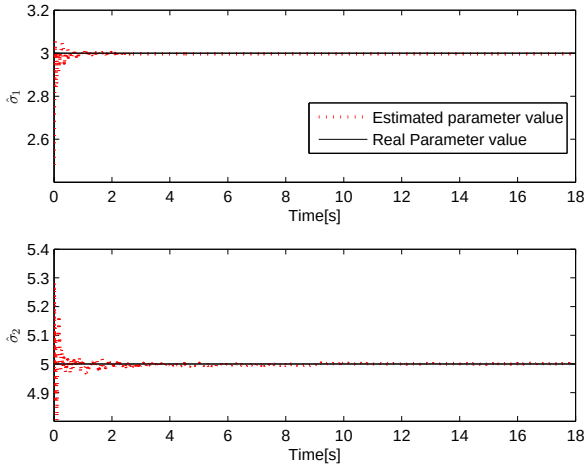


Fig. 6. $\alpha_1$ and $\sigma_1^2$ estimation performance a realization on AP5.

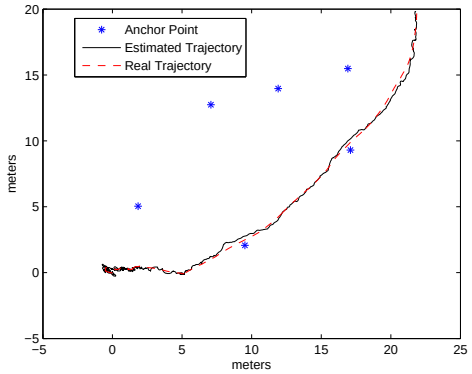


Fig. 7. Real mobile trajectory versus estimated trajectory.


[2] David I. Laurenson, *Indoor Radio Channel Propagation Modelling by Ray Tracing Techniques*, PhD dissertation, University of Edinburgh, 1994.

[3] T. Jamsa, T. Poutanen, and J. Meinila, "Implementation Techniques of Broadband Radio Channel Simulators," in *Vehicular Technology Conference, 2001. VTC 2001 Spring. IEEE VTS 53rd*, 2001, vol. 1, pp. 433–437 vol.1.

[4] M.A. Assad, M. Heidari, and K. Pahlavan, "Effects of Channel Modeling on Performance Evaluation of WiFi RFID Localization Using a Laboratory Testbed," in *Global Telecommunications Conference, 2007. GLOBECOM '07. IEEE*, 2007, pp. 366–370.

[5] T. Paul and T. Ogunfunmi, "Wireless LAN Comes of Age: Understanding the IEEE 802.11n Amendment," *Circuits and Systems Magazine, IEEE*, vol. 8, no. 1, pp. 28–54, 2008.

[6] E. Mazor, A. Averbuch, Y. Bar-Shalom, and J. Dayan, "Interacting multiple model methods in target tracking: a survey," *Aerospace and Electronic Systems, IEEE Transactions on*, vol. 34, no. 1, pp. 103–123, Jan 1998.

[7] Emil Semerdjiev Ludmila Mihaylova, "An interacting multiple model algorithm for stochastic systems control," *Information and security. And international journal*, vol. 2, pp. 102–112, 1999.

[8] Bor-Sen Chen, Chang-Yi Yang, Feng-Ko Liao, and Jung-Feng Liao, "Mobile location estimator in a rough wireless environment using extended kalman-based imm and data fusion," *Vehicular Technology, IEEE Transactions on*, vol. 58, no. 3, pp. 1157–1169, March 2009.

[9] Chen and Bajpai D., "Improving time-to-collision estimation by imm based kalman filter," *SAE Technical Paper*, 2009.

[10] L. Schumacher V. Erceg, "TGn channel models. IEEE 802.11 Wireless LANs Document," *IEEE 802.11-03/940r4*, May, 2004.

[11] H. Hashemi, "The Indoor Radio Propagation Channel," *Proceedings of the IEEE*, vol. 81, no. 7, pp. 943–968, 1993.

[12] A.R. Sandeep, Y. Shreyas, Shivam Seth, Rajat Agarwal, and G. Sadashivappa, "Wireless Network Visualization and Indoor Empirical Propagation Model for a Campus Wi-Fi Network," *World Academy of Science, Engineering and Technology*, vol. 18, no. 6, pp. 705 – 710, 2008.

[13] N. Patwari, A.O. Hero, M. Perkins, N.S. Correal, and R.J. O'Dea, "Relative Location Estimation in Wireless Sensor Networks," *Signal Processing, IEEE Transactions on*, vol. 51, no. 8, pp. 2137–2148, 2003.

[14] A.J. Coulson, A.G. Williamson, and R.G. Vaughan, "A Statistical Basis for Lognormal Shadowing Effects in Multipath Fading Channels," *Communications, IEEE Transactions on*, vol. 46, no. 4, pp. 494–502, 1998.

[15] M.A. Caceres, F. Sottile, and M.A. Spirito, "Adaptive location tracking by kalman filter in wireless sensor networks," in *Wireless and Mobile Computing, Networking and Communications, 2009. WIMOB 2009. IEEE International Conference on*, Oct 2009, pp. 123–128.

[16] R. Mehra, "Approaches to adaptive filtering," *IEEE Trans. on Automatic Control*, vol. 17, no. 10, pp. 693–698, 1972.

[17] M. Šimandl and J. Duník, "Multi-step prediction and its application for estimation of state and measurement noise covariance matrices," Tech. Rep., Dep. of Cybernetics, University of West Bohemia, Pilsen, Czech Republic, 2006.

[18] K. A. Myers and B. D. Tapley, "Adaptive sequential estimation with unknown noise statistics," *IEEE Trans. on Automatic Control*, vol. 21, no. 8, pp. 520–523, 1976.

[19] I. Blanchet and C. Frankignoul, "A comparison of adaptive Kalman filters for a tropical pacific ocean model," *Monthly Weather Review*, vol. 125, pp. 40–58, 1997.